Lab on a Chip

RSC Publishing

PAPER

View Article Online
View Journal | View Issue



Cite this: *Lab Chip*, 2013, **13**, 2397

# Simple, distance-based measurement for paper analytical devices

David M. Cate,[a] Wijitar Dungchai,[b] Josephine C. Cunningham,[c] John Volckens*[ad] and Charles S. Henry*[ac]

Received 15th January 2013,
Accepted 25th April 2013

DOI: 10.1039/c3lc50072a

**www.rsc.org/loc**

Paper-based analytical devices (PADs) represent a growing class of elegant, yet inexpensive chemical sensor technologies designed for point-of-use applications. Most PADs, however, still utilize some form of instrumentation such as a camera for quantitative detection. We describe here a simple technique to render PAD measurements more quantitative and straightforward using the distance of colour development as a detection motif. The so-called distance-based detection enables PAD chemistries that are more portable and less resource intensive compared to classical approaches that rely on the use of peripheral equipment for quantitative measurement. We demonstrate the utility and broad applicability of this technique with measurements of glucose, nickel, and glutathione using three different detection chemistries: enzymatic reactions, metal complexation, and nanoparticle aggregation, respectively. The results show excellent quantitative agreement with certified standards in complex sample matrices. This work provides the first demonstration of distance-based PAD detection with broad application as a class of new, inexpensive sensor technologies designed for point-of-use applications.

## Introduction

Methods to measure chemical composition, a fundamental need in virtually all science and engineering disciplines, have undergone rapid technological development in recent years. For example, single gene analyses that once took days to complete can now be conducted in minutes using instruments that quantify thousands of genes simultaneously. Most technological advancements in the field of measurement science focus on increasing sample throughput, and/or reducing sample detection limit.[1–7] While such technological advancements have enhanced our understanding of chemistry and biology, they are often limited to laboratory use by highly trained scientists. Consequently, there is a growing recognition of the need to augment powerful modern analytical tools with low-cost methods designed for point-of-use applications.[8–11]

Point-of-use measurement technologies are often simple and inexpensive but sacrifice detection limit and operating range for sensitivity, specificity, and speed.[12–16] Point-of-use technologies are also attractive because they are low cost and require minimal user training. Such technologies can have great impact on science and also in society. Examples include simple and elegant technologies such as litmus paper or the home pregnancy test, both of which have diffused far into everyday societal contexts. Common to each of these point-of-use devices is their reliance on simple capillary-based flow for the analytics.

Paper-based analytical devices, first introduced by the Whitesides group in 2007, are a type of point-of-use technology that uses porous cellulose (*i.e.*, common filter paper) to store reagents and the addition of water to generate flow *via* capillary action.[17] Hydrophobic materials printed onto paper define circuits that control the flow path.[16,18–21] Unlike traditional analytical techniques making use of paper as a substrate, the use of patterning in these devices increases the overall functionality. To conduct chemical analysis, colorimetric reagents are added to specific zones within the paper, with analyte detection and quantification carried out by changes in colour hue and/or intensity.[16] Although straightforward, this detection method has limitations, including user variability when distinguishing changes in reagent hue and intensity.[22–26] Consequently, even with PADs, precise and accurate quantification can require the use of peripheral technologies such as digital scanners, cameras, or other optical techniques.[16,26,27] Instrumented techniques, such as electrochemistry, can also help improve PAD performance.[28–30] Ladder-based barcode assays have also been developed which reduce the requirement for color differentiation by the user.[31–34]

[a]*Department of Biomedical Engineering, Colorado State University, Fort Collins, CO 80523, USA*
[b]*Department of Chemistry, Faculty of Science, King Mongkut's University of Technology, Thonburi Bangkok 10140, Thailand*
[c]*Department of Chemistry, Colorado State University, Fort Collins, CO 80523, USA. E-mail: chuck.henry@colostate.edu*
[d]*Department of Environmental and Radiological Health Sciences, Colorado State University, Fort Collins, CO 80523, USA. E-mail: john.volckens@colostate.edu*

We present here a simplified technique for quantitative PAD detection with broad chemical applicability, referred to as distance-based detection or chemometer. In this approach, colorimetric reagents, designed to precipitate or aggregate upon reaction with the analyte, are deposited along the capillary flow path. Consequently, as flowing analyte reacts with reagent, colour develops along the flow line until all of the analyte is consumed. Quantification is achieved by measuring colour *length*, thus eliminating the need to differentiate hues and intensities by the user (as is typical with existing PAD devices). Measuring length instead of colour intensity produces fewer user errors from device to device and renders the analytical measurement largely independent of the operator.

Distance-based detection on paper has been demonstrated previously. Zuk *et al.* quantified theophylline levels in whole blood and serum by distance-based detection using antibody-activated chromatography paper.[35,36] Since then, few applications have been reported using this detection motif.[37,38] In 1990, Allen and co-workers developed a similar enzyme-based method for measuring cholesterol levels on paper.[39] Chatterjee *et al.* developed a PDMS microfluidic device using biotin-modified channels and flow distance as the detection motif for fluorescently labelled streptavidin.[27] A complementary strategy was recently demonstrated by Lewis *et al.* for point-of-care (POC) paper-based detection using individual strips of paper that turn colour in response to the presence of an analyte. Quantification is determined by counting the number of strips that turn colour.[40]

Our method extends distance-based detection on paper beyond the use of immobilized enzymes and antibodies. The method presented here is simplified and broadened in scope; our method requires fewer steps to complete the analysis and may be applied to a broader class of analytes. In addition, our use of wax printed devices (*vs.* paper strips) is amenable to multiplexing. Because our method couples the cost effectiveness and simplicity of printed hydrophobic barriers, our paper devices would also scale well for mass fabrication. This form of distance-based PAD detection can be applied to analytes beyond the biotinylation and immunoassays described previously.

In this work, we demonstrate non-instrumented analysis using distance-based detection of a broad range of analytes using three different detection motifs: nanoparticle aggregation, metal complexation, and enzymatic activity. To demonstrate the utility of our method, we developed assays for detection of nickel, reduced glutathione (GSH), and glucose. These three analytes represent compounds found in environmental (Ni) and biological (GSH, glucose) samples. Chronic or even acute exposure to Ni is associated with a number of toxic effects.[41–44] Glutathione is an endogenous marker of oxidative stress and can impart useful information about the health of an individual.[45–49] Glucose monitoring is essential for controlling blood sugar levels in diabetic patients. Analyte measurements were accurate and precise, with detection sensitivities for Ni, GSH, and glucose of 0.7 μg $m^{-3}$, 0.12 nmol, and 11 mg $dL^{-1}$ respectively. Once developed, the distance-based PADs were used to quantify each analyte in a relevant biological or environmental sample. We found no significant difference in measured values when samples with known analyte concentration were tested with each device, demonstrating the applicability of this method to real-world samples.

## Experimental methods

### Materials and equipment

Glutathione (reduced form), glutathione disulfide, cystine, cysteine, and homocysteine, dimethylglyoxime (DMG), sodium acetate trihydrate, and sodium fluoride (0.5 M), D-(+)-glucose, glucose oxidase (GOx, from *Aspergillus niger*, 5 U $mg^{-1}$) and peroxidase Type I (HRP, from *Horseradish*, 100 U $mg^{-1}$) were purchased from Sigma-Aldrich (St. Louis, MO). The silver nanoparticle solution (AgNPs) was obtained from the Sensor Research Unit at the Department of Chemistry, Chulalongkorn University, Thailand. Tris-hydrochloride and ammonium hydroxide were purchased from Mallinckrodt Baker, Inc. (Phillipsburg, NJ). Glacial acetic acid and potassium phosphate were purchased from Fisher Scientific (Pittsburgh, PA). Nitric acid (18.4 M) was purchased from EMD Millipore (Billerica, MA, USA). The 3,3′-diaminobenzidine (DAB) in peroxidase substrate kit was obtained from Vector Laboratories, Inc. (Burlingame, CA). All chemicals were used as received without further purification. An industrial incineration ash sample (*RTC*-CRM012-100) certified for heavy metals content was obtained from LGC Standards (Teddington, UK). Whatman No. 1 qualitative-grade filter paper was purchased from General Electric Company (Schenectady, New York). CorelDraw and Adobe Illustrator software were used to design the hydrophobic wax barrier for all three assay types. Hydrophobic wax barriers were printed on filter paper using a commercial wax printer (Xerox Colorqube 8870).

### Device operation

The operational concept is shown in Fig. 1 along with three detection chemistries selected to demonstrate application pathways. The microfluidic flow circuit, which closely resembles a thermometer, is designed using graphics software and printed onto standard cellulosic filter paper using wax ink. A circular reservoir at the bottom accommodates sample addition; filter paper in the reservoir may be retained (*e.g.*, to hold reagents for sample pre-treatment) or removed to facilitate sample transfer into the detection zone. Colorimetric detection reagents are deposited along the flow channel by spray application or pipetting. Spray application uses a nebulizer to deposit reagent droplets uniformly along the channel. This process is fast but inefficient, as significant amounts of reagent are deposited onto the surrounding paper (outside the flow circuit). Reagents in the surrounding paper do not, however, affect experimental results because they are separated from the flow channel by a wax barrier. Alternatively, reagents may be pipetted onto the paper in minute (0.5 μL)

 

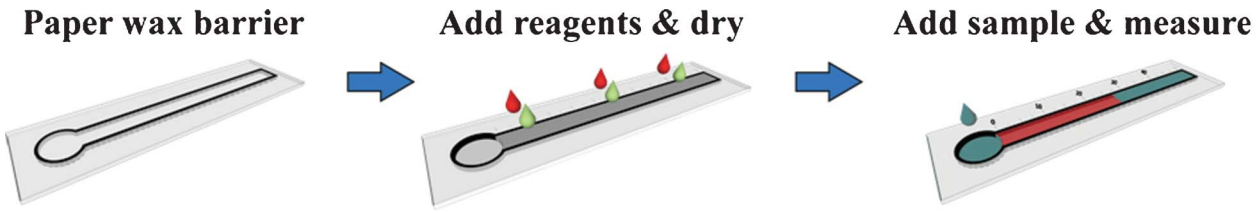


**Fig. 1** Operational concept of the device. Device fabrication and use are simple, inexpensive, and fast, consisting of printing a hydrophobic barrier on filter paper, patterning reagents, and adding a sample for analysis.



increments. This process consumes less reagent but is somewhat tedious and time-intensive. Once the reagents are dry, the device is ready for use. An aqueous sample extract is added to the sample reservoir and then carried by capillary action along the flow channel. As the analyte reacts with its reagent, a coloured product develops. Once all of the analyte is consumed, the colour development stops (even though eluent proceeds to wick along the channel). Analyte quantification is then as simple as measuring the length of the coloured region in the flow channel, typically with a ruler that can either be held up to or printed directly along the channel for user-friendliness and portability. No computer software is required for analyte quantification. A desktop scanner and computer software (Xerox DocuMate 3220 Scanner, colour photo setting, 600 dpi) were also used to quantify colour distance but only for the purpose of experimental validation.

After adding an analyte/eluent mixture to the sample zone of the device, assay measurement is performed once the eluent completely evaporates (~15–20 min), however a reading could be accomplished in less than 10 min once the channel becomes completely saturated and the flow velocity becomes negligible. In the 10 min needed for the eluent to reach the end of the channel, all upstream colour formation (*i.e.* analyte complexes with reagents) has already taken place.

The flow Reynolds number along the sample channel is low (~10), favouring laminar flow along the channel. The parabolic flow front was unexpected (Washburn flow in porous materials exhibits a flattened velocity profile) but may be due to interactions with the wax at the edges of the channels. Colour distance is measured from the beginning of the channel near the sample zone to the most downstream tip of detectable colour (*i.e.*, the apex of the parabolic flow profile). Albeit somewhat arbitrary, the tip of colour was chosen for detection instead of the farthest colour region spanning the width of the channel because both methods provide approximately the same level of reproducibility (6.1 and 6.5% RSD respectively), and the difference in analyte concentration in choosing one method over the other is lower than the limit of quantification for each assay (data not shown). We chose to measure to the tip of colour formation because it improves detection sensitivity the most.

### Glutathione detection

The paper assay for glutathione detection consisted of a circular reservoir for sample addition (6 mm diameter) and a baffled flow channel (3 × 60 mm) divided into 14 equal sections (0.3 × 2 mm). The flow baffles were used to decrease the capillary flow velocity along the channel, maximizing reaction time between glutathione and the AgNPs. The AgNP solution (0.5 μL) was spotted onto each of the 14 sections along the channel. For each assay, 20 μL of sample solution was added to the sample reservoir. Complete sample analysis took approximately 10 min. Assay selectivity was investigated by addition of 20 μL of standard thiol solution (0.5 nmol), which did not form a coloured reaction product along the paper channel.

### Glucose detection

The paper-based assay for glucose detection consisted of a wax-printed circular reservoir (5 mm diameter) for GOx and HRP enzyme modification and a straight channel (2 × 40 mm) for measuring glucose reaction with peroxidase and DAB. Aliquots (0.5 μL) of 600 U $mL^{-1}$ GOx and 500 U $mL^{-1}$ HRP were spotted on the sample reservoir and 0.5 μL of DAB was pipetted onto the straight channel every five millimeters to account for reagent spreading along the channel length. For each assay, 20 μL of the standard or sample solution was added to the sample reservoir.

**Analysis of glutathione and glucose in human serum.** Human control serum samples (levels I and II) for both GSH and glucose were obtained from Pointe Scientific (Canton, MI). Levels of analytes were provided by the supplier. Before analysis, unwanted protein was removed by filtration (10 KDa MWCO) and centrifugation at 10 000 rpm for 20 and 10 min, respectively, for glucose and GSH. A solution of 5% 5-sulfosalicylic acid was added prior to centrifugation for GSH.

### Nickel detection

A nebulizer was used to saturate the paper surface with DMG (50 mM). The deposited reagents were then air dried. The paper was uniformly coated with ammonium hydroxide (pH 9.5) because the rate and extent of $Ni^{2+}$-DMG complexation are pH dependent with the fastest rate occurring at pH 9. To prevent user contamination and excess solvent evaporation, the filter paper was passed through a desktop laminator at 150 °C (Model No. 92499, Gordon) twice on each side. Laminating the paper also provided better mechanical stability for assay handling. A 6.4 mm (ID) hole was punched through the sample reservoir and masking tape was applied to one side to prevent sample loss from leakage during use. For analysis, 20 μL of a Ni standard solution (1000 ppm) was deposited onto the sample reservoir. The Ni-DMG complex is reddish pink and precipitates upon formation. Colour development is rapid and total sample analysis was performed in <10 min.

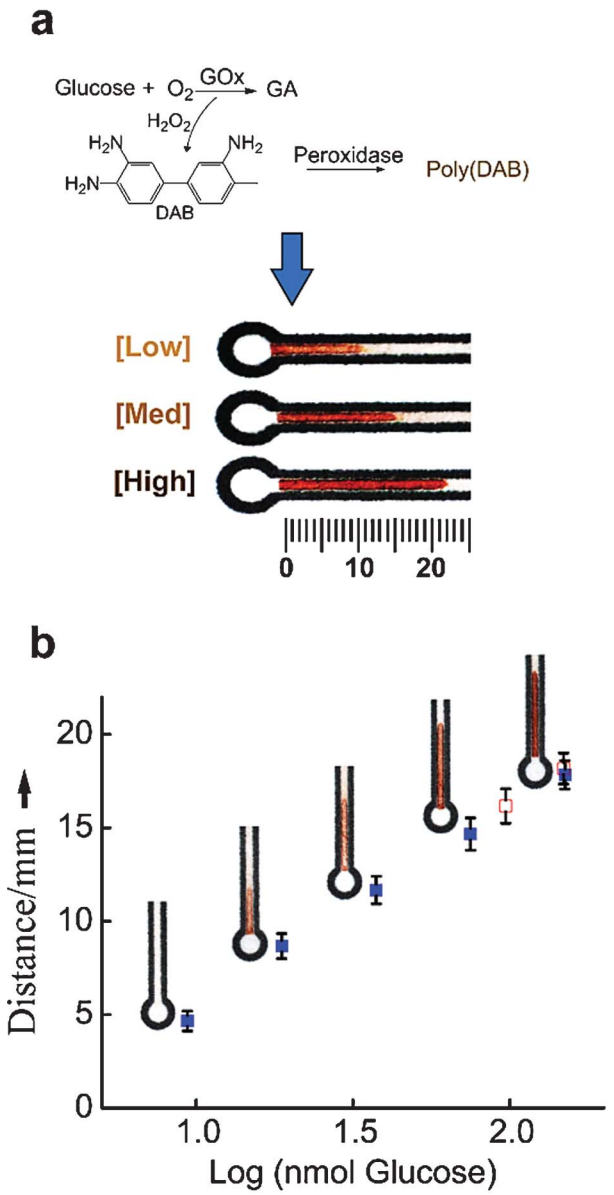


**Fig. 2** (a) Glucose oxidase reacts with DAB and peroxidase to form a brown precipitate in approximately five minutes. (b) Analyte flow of standard solutions compared with real (complex) serum samples. Standard curves show the distance of color development is proportional to the amount of glucose added (closed blue squares). The extent of the reaction is easily visualized within the linear range of the reaction. Photos of the complete reaction are included for each calibration data point. Reaction distance for complex serum samples (open red squares) show good agreement with standard calibration curves (closed blue squares). Error bars represent one standard deviation ($n$ = 6).

**Analysis of Ni in combustion incineration ash.** An incineration ash sample was purchased for assay validation. Briefly, incineration ash along with 1 mL concentrated nitric acid was heated in a 20 mL scintillation vial for 5 min at ~250 °C on a hotplate until complete acid evaporation. A 262 μL solution containing deionized water (250 μL), sodium fluoride, acetic acid (2 : 1 : 1 v/v%), and 12 μL sodium hydroxide (12 M) was added to the vial. After homogenous mixing with a pipette for several seconds, the solution was centrifuged for 10 min at 14 000 RPM. For each assay, 20 μL of the supernatant was added to the sample reservoir.

## Results and discussion

### Glucose quantification

Detection of glucose is shown in Fig. 2a using glucose oxidase, 3,3′-diaminobenzidine (DAB) and peroxidase. In this reaction, glucose oxidase produces hydrogen peroxide that further reacts with DAB in the presence of peroxidase to form a brown, insoluble product (polyDAB). DAB is colourless but forms a highly coloured and easily visualized product after reacting with the analyte.

To demonstrate method viability, levels of glucose in a serum standard were quantified. Test results, along with device photographs, are shown in Fig. 2b (calibration data is shown as blue squares). The plot depicts sample reaction length as a logarithmic function of the known analyte concentration. For glucose detection, the length of the coloured range is proportional to the amount of glucose added over the range of 7 to 200 nmol. Negative controls (zero sample concentration) produced no discernible colour change (data not shown). The linear range obtained for glucose in our system is approximately 11–270 mg $dL^{-1}$, having a slightly lower detection limit than commercially available point-of-care blood glucose meters (~20 mg $dL^{-1}$).[50] The upper range in our system is limited however, and is approximately half the level of commercial systems (500 mg $dL^{-1}$).

Method variability is relatively low as seen by the small error bars (representing standard deviations of repeat measures) around each datum. We tested this system using serum samples known to contain either normal or abnormal glucose levels. Such commercially-available control samples are widely used for assay validation because they have all the complexity of normal serum without the worry of blood-borne pathogens. Glucose concentrations within the control serum samples are shown as open red squares; their alignment with the calibration curve shows the ability of this method to measure glucose accurately and precisely in a relatively complex sample matrix.

### Quantification of nickel in a combustion ash sample

Detection of nickel ($Ni^{2+}$) using dimethylglyoxime (DMG) as an example assay for toxic metals is shown in Fig. 3a. In this assay, DMG is placed in the channel and reacts with $Ni^{2+}$ to form a pinkish-red product. $Ni(DMGH)_2$ is poorly soluble and immediately precipitates from solution. Solutions containing $Ni^{2+}$ are colourless in the absence of DMG. For Ni detection, the concentration that linearly corresponds to colour length is 0.7–92 μg $m^{-3}$. The legal limit for exposure to Ni in occupational settings is 1000 μg $m^{-3}$, for which our detection limits are clearly sufficient.[34] We are continuing to investigate methods for improving the dynamic range of the assay. We envision this test could develop into a very cost effective, 'first-pass' evaluation tool for personal exposure to aerosol pollution containing Ni compounds. We next established the sensitivity of the assay to the amount of DMG deposited on the device

 

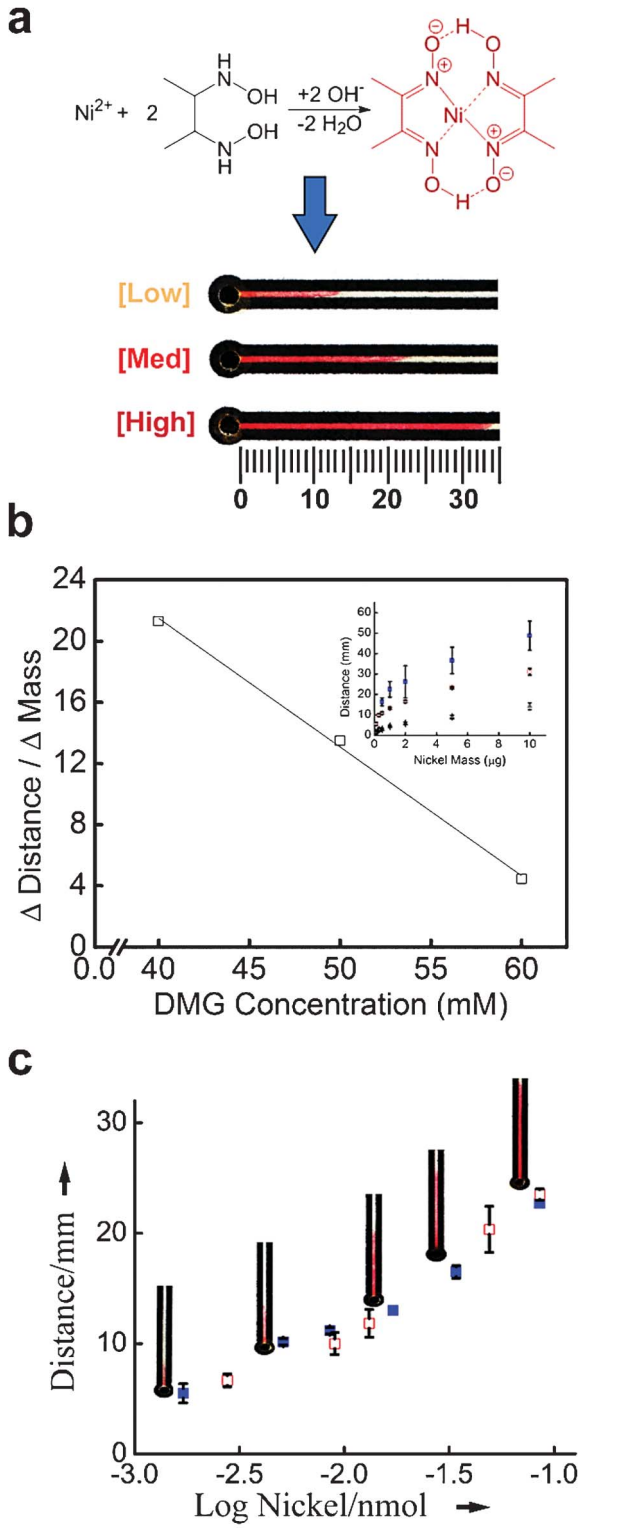


**Fig. 3** (a) Formation of a bright red precipitate is easily visualized when DMG-$Ni^{2+}$ complexation occurs. The reaction product is formed immediately, and complete analysis in the concentration range studied took approximately 15 min. (b) Assay sensitivity decreases as the concentration of DMG increases. [Inset] The limit-of-detection (LOD) for the Ni assay increases as the concentration of DMG increases from 40 mM (closed blue squares) to 50 mM (open red squares) to 60 mM (closed grey triangles). (c) Standard curves show the distance of color development is proportional to the amount of Ni added (closed blue squares). A sample of incineration ash was tested for method validation (open red squares). Error bars represent one standard deviation ($n$ = 8).

(Fig. 3b). As the amount of DMG increases, the sensitivity of the assay decreases. The assay can detect nmol levels of $Ni^{2+}$ in the presence of other transition and heavy metals making it useful for a range of application areas from water analysis to particulate matter composition studies.[51]

Levels of aqueous $Ni^{2+}$ concentrations were evaluated in a certified combustion incineration ash sample as part of an on-going program to develop fast, inexpensive environmental measurement tools. Combustion incineration ash is a by-product of medical, municipal, and industrial incineration processes and can be a significant contributor to local and regional air, water, and soil pollution. For this assay, DMG was deposited uniformly along the flow channel and solutions containing known amounts of nickel (in 20 μL aliquots), first dissolved in concentrated $HNO_3$, were added to the inlet to prepare calibration curves. The Ni-DMG complex gave a highly coloured product that was readily distinguished from the clear sample solution.[52] Various dilutions of the resulting solution were analyzed and the results shown as open red squares in Fig. 3c. Good agreement was obtained between measured and known Ni concentrations showing the ability of the chem-ometer method to carry out these measurements in complex sample matrices.[41] Our lab continues to evaluate strategies for mobilizing the acid digestion process. The colour intensity that developed down the paper channel remained essentially constant. This was unexpected since we assumed the colour intensity would soften as the Ni remaining in solution reacted with DMG. One possible explanation for this phenomenon is that $Ni(DMGH)_2$ becomes highly concentrated in a confined space on the paper (solvent evaporation drives this process) causing irregular particle clusters to form, which saturates the surface. No discernible colour changes or reaction products were observed in negative controls.

### GSH quantification assay

Detection of GSH using a silver nanoparticle (AgNP) aggregation assay is shown in Fig. 4a. In this assay, AgNPs aggregate in the presence of GSH to form a reddish-brown product that is distinguished from the orange colour of the AgNPs in the absence of glutathione. AgNPs (11 nm diameter) were spotted onto the detection channel, turning it a dark orange colour. These nanoparticles aggregate in the presence of glutathione, which causes a colour shift from orange to deep red on the paper (Fig. 4b).[53] The filled blue squares represent calibration data of known GSH concentration. A colour change from orange to light orange was also observed when only buffer was added. The buffer effect, however, was easily distinguished from the dark red of the glutathione specific product. The shift in absorbance maximum in the presence of buffer is hypothesized to result from weak non-specific aggregation of the AgNPs.

The ability to measure glutathione spiked in serum samples (open red squares in Fig. 4b) was also determined. As can be seen, the distances measured with serum samples (4.2 and 5.7 mm) agree well with those of the standard solutions (3.7 and 5.3 mm) for glutathione concentrations 0.25 and 0.5 nmol, respectively (Table 1). Detection of glutathione was log-linear for the concentration range tested (0.12–2.0 nmol). The detection limits for this assay are on the same order as

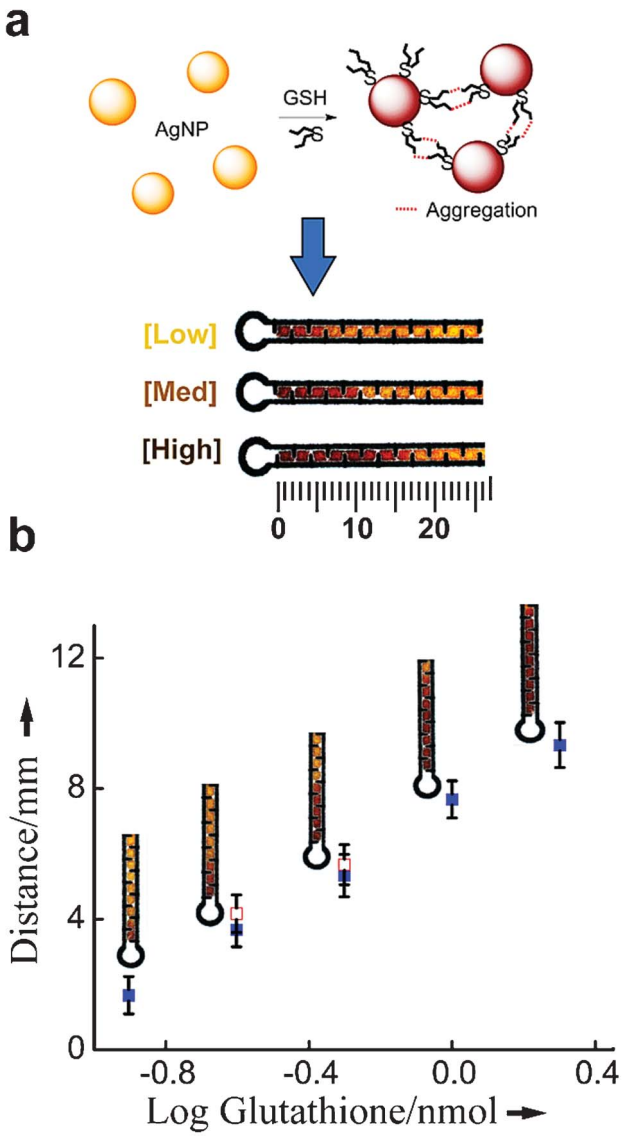


**Fig. 4** (a) AgNPs aggregate in the presence of glutathione and produce a reddish-brown color, easily distinguishable by the naked eye. Reaction kinetics were slow, so wax baffles were used to divert flow in a serpentine pattern as capillary action flowed liquid through the channel. For one assay, the detection of glutathione within the concentration range tested took approximately 10 min. (b) Standard curves show the distance of color development is proportional to the amount of glutathione added (blue squares). Spiked serum samples were evaluated for method validation (open red squares). Error bars represent one standard deviation ($n$ = 4).

conventional measurement methods for GSH, however the dynamic range for the most sensitive assays extends a few orders of magnitude higher.

The assay selectivity against other thiols (cysteine and homocysteine) and disulfides (cystine, homocystine, and glutathione disulfide) was also investigated (Fig. 5). Cysteine and homocysteine did cause a similar colour change but the length of colour development was much less than for glutathione. None of the disulfides tested produced any colour change.

For all three assays, colour formation and bulk flow along the channel was observed to follow the Lucas–Washburn equation for flow in capillary tubes (data not shown). Reaction kinetics for each assay was assumed to be rapid compared with solvent flow rate, so the length of colour production along a channel is driven only by flow rate.

We have demonstrated this method using three representative compounds commonly found in environmental and biological matrices, but this method should be easily extendable to a much larger range of analytes because of the possibility for cellulose modification.[54] Even without substrate modification, our detection motif is applicable for analysis of a variety of transition and heavy metals, including Fe, Mn, Cr, Cu, Hg, and Pb. Many biological compounds should also be quantifiable with this method *via* nanoparticle aggregation, including lysine, heparin, thrombin, and DNA.[55–59]

## Conclusions

The distanced-based detection concept represents a new and dramatically simplified technique for quantitative PAD detection that eliminates peripheral instrumentation during sample analysis. This technology is adaptable to suit different detection chemistries and multiple analytes, including those from complex environmental and biological matrices where analyte specificity is critical. One challenge that must be overcome with our method is the current requirement for the sample to be solubilized; however we are developing new methods of analysis that will accommodate samples in multiple formats and with various solvents. The assays described herein were developed in controlled laboratory conditions with small variability in temperature and relative humidity (25 °C and ~30%RH), however if studies were conducted in a less controllable environment (*i.e.* for environmental monitoring), large changes in ambient conditions could affect wicking velocity and alter results. We plan to further investigate these and other variables to improve assay reproducibility in a wider range of ambient conditions.

Paper-based analytical devices hold great potential for application at the point-of-use. The analytical technique presented here is minimally instrumented for device portability and is highly cost effective; excluding fabrication equipment (computer, drawing software, printer, pipette), a single assay costs approximately $0.04.[51] Since analyte quantification is immediate and can be performed on-site, processing time is dramatically reduced when compared to other centralized measurement techniques, which often sacrifice processing speed for detection sensitivity. Like most PAD technologies, this technique sacrifices dynamic range for cost, speed, and ease of use. However, we have shown that devices can be tuned to detect different analyte concentration ranges by modulating reagent concentrations in the flow channel, thus, accommodating different reaction stoichiometries.

Chemical measurement technologies such as the home pregnancy kit or blood glucose meter have revolutionized personal healthcare. Similarly, alternative low-cost strategies

 

**Table 1** Determination of glucose and glutathione in human serum ([a]SD: standard deviation, $n = 3$).

| Real samples | Concentration ([a]SD, standard deviation ($n = 3$)) | | |
|---|---|---|---|
| Glucose | Certified value (mM ± SD[a]) | Measured (mM ± SD[a]) | %Recovery |
| Serum level 1 | 5.6 ± 0.4 | 6.1 ± 0.2 | 108.7 |
| Serum level 2 | 16.8 ± 1.7 | 18.6 ± 0.3 | 110.8 |
| Glutathione | Added (μM) | Measured (μM ± SD[a]) | %Recovery |
| Spiked serum 1 | 6.2 | 7.1 ± 2.5 | 112.9 |
| Spiked serum 2 | 12.5 | 13.4 ± 0.0 | 107.3 |
| Spiked serum 3 | 25.0 | 21.1 ± 2.9 | 84.2 |

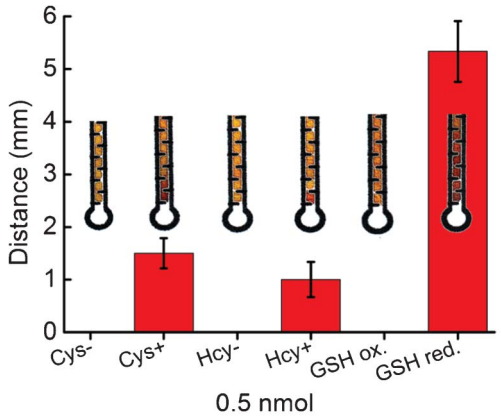


**Fig. 5** Selectivity study of AgNPs aggregation for glutathione determination against other thiols: cystine (Csy−), cysteine (Cys+), homocystine (Hcy−), homocysteine (Hcy+), and glutathione oxidized form at 0.5 nmol. Error bars represent one standard deviation ($n = 3$).

are being developed for environmental applications. We have presented a technology that can be applied for rapid, on-site detection of targeted analytes, which is critical for understanding sources, transformations, and fates of environmental contaminants. This technology represents a step towards empowerment of the 'citizen scientist' – the idea that people will not only be able to monitor their exposure to harmful pollutants on a personal level, but can rapidly identify sources of pollution for further scientific evaluation and remediation.

## Acknowledgements

This work was supported by grants from the National Institute for Occupational Safety and Health (OH010050) and the National Institute of Environmental Health Sciences (ES019264).

## References

1 E. Bakker and E. Pretsch, *TrAC, Trends Anal. Chem.*, 2005, **24**, 199–207.
2 B. S. Broyles, S. C. Jacobson and J. M. Ramsey, *Anal. Chem.*, 2003, **75**, 2761–2767.
3 R. Fan, O. Vermesh, A. Srivastava, B. K. H. Yen, L. Qin, H. Ahmad, G. A. Kwong, C.-C. Liu, J. Gould, L. Hood and J. R. Heath, *Nat. Biotechnol.*, 2008, **26**, 1373–1378.
4 S. P. FitzGerald, J. V. Lamont, R. I. McConnell and E. O. Benchikh, *Clin. Chem.*, 2005, **51**, 1165–1176.
5 J. A. Hansen, J. Wang, A.-N. Kawde, Y. Xiang, K. V. Gothelf and G. Collins, *J. Am. Chem. Soc.*, 2006, **128**, 2228–2229.
6 G. Huang, Z. Ouyang and R. G. Cooks, *Chem. Commun.*, 2009, 556–558.
7 A. H. Merrill Jr, M. C. Sullards, J. C. Allegood, S. Kelly and E. Wang, *Methods*, 2005, **36**, 207–224.
8 T. Dworak, C. Gonzalez, C. Laaser and E. Interwies, *Environ. Sci. Policy*, 2005, **8**, 301–306.
9 A. E. Herr, A. V. Hatch, W. V. Giannobile, D. J. Throckmorton, H. M. Tran, J. S. Brennan and A. K. Singh, *Ann. N. Y. Acad. Sci.*, 2007, **1098**, 362–374.
10 N. Maisonneuve, M. Stevens, M. E. Niessen, L. Steels, I. N. Athanasiadis, A. E. Rizzoli, P. A. Mitkas and J. M. Gómez, *NoiseTube: Measuring and mapping noise pollution with mobile phones*, Springer, Berlin Heidelberg, 2009, pp. 215–228.
11 P. von Lode, *Clin. Biochem.*, 2005, **38**, 591–606.
12 S. J. Barnes and E. Scornavacca, *International Journal of Mobile Communications*, 2004, **2**, 128–139.
13 S. F. Clarke and J. R. Foster, *Br. J. Biomed. Sci.*, 2012, **69**, 83–93.
14 S. Kanji, J. Buffie, B. Hutton, P. S. Bunting, A. Singh, K. McDonald, D. Fergusson, L. A. McIntyre and P. C. Hebert, *Crit. Care Med.*, 2005, **33**, 2778–2785 2710.1097/2701.CCM.0000189939.0000110881.0000189960.
15 I. Korhonen, J. Parkka and M. Van Gils, *IEEE Eng. Med. Biol. Mag.*, 2003, **22**, 66–73.
16 A. W. Martinez, S. T. Phillips, E. Carrilho, S. W. Thomas, H. Sindi and G. M. Whitesides, *Anal. Chem.*, 2008, **80**, 3699–3707.
17 A. W. Martinez, S. T. Phillips, M. J. Butte and G. M. Whitesides, *Angew. Chem., Int. Ed.*, 2007, **46**, 1318–1320.
18 D. A. Bruzewicz, M. Reches and G. M. Whitesides, *Anal. Chem.*, 2008, **80**, 3387–3392.
19 E. Carrilho, A. W. Martinez and G. M. Whitesides, *Anal. Chem.*, 2009, **81**, 7091–7095.
20 W. K. T. Coltro, D. P. de Jesus, J. A. F. da Silva, C. L. do Lago and E. Carrilho, *Electrophoresis*, 2010, **31**, 2487–2498.
21 Y. Lu, W. Shi, L. Jiang, J. Qin and B. Lin, *Electrophoresis*, 2009, **30**, 1497–1500.
22 T. Songjaroen, W. Dungchai, O. Chailapakul, C. S. Henry and W. Laiwattanapaisal, *Lab Chip*, 2012, **12**, 3392–3398.

23 A. K. Ellerbee, S. T. Phillips, A. C. Siegel, K. A. Mirica, A. W. Martinez, P. Striehl, N. Jain, M. Prentiss and G. M. Whitesides, *Anal. Chem.*, 2009, **81**, 8447–8452.
24 J. C. Jokerst, J. A. Adkins, B. Bisha, M. M. Mentele, L. D. Goodridge and C. S. Henry, *Anal. Chem.*, 2012, **84**, 2900–2907.
25 M. P. Allen, A. DeLizza, U. Ramel, H. Jeong and P. Singh, *Clin. Chem.*, 1990, **36**, 1591–1597.
26 W. Zhao, M. M. Ali, S. D. Aguirre, M. A. Brook and Y. Li, *Anal. Chem.*, 2008, **80**, 8431–8437.
27 D. Chatterjee, D. S. Mansfield, N. G. Anderson, S. Subedi and A. T. Woolley, *Anal. Chem.*, 2012, **84**, 7057–7063.
28 A. Apilux, W. Dungchai, W. Siangproh, N. Praphairaksit, C. S. Henry and O. Chailapakul, *Anal. Chem.*, 2010, **82**, 1727–1732.
29 W. Dungchai, O. Chailapakul and C. S. Henry, *Anal. Chem.*, 2009, **81**, 5821–5826.
30 Z. Nie, C. A. Nijhuis, J. Gong, X. Chen, A. Kumachev, A. W. Martinez, M. Narovlyansky and G. M. Whitesides, *Lab Chip*, 2010, **10**, 477–483.
31 J.-H. Cho and S.-H. Paek, *Biotechnol. Bioeng.*, 2001, **75**, 725–732.
32 C. Fang, Z. Chen, L. Li and J. Xia, *J. Pharm. Biomed. Anal.*, 2011, **56**, 1035–1040.
33 K.-K. Fung, C. P.-Y. Chan and R. Renneberg, *Anal. Chim. Acta*, 2009, **634**, 89–95.
34 K.-K. Fung, C.-Y. Chan and R. Renneberg, *Anal. Bioanal. Chem.*, 2009, **393**, 1281–1287.
35 R. F. Zuk, V. Ginsberg, K. T. Houts, R. Judith, H. Merrick, E. F. Ullman, M. M. Fischer, C. C. Sizto, S. N. Stiso and D. J. Litman, *Clin. Chem.*, 1985, **31**, 1144–1150.
36 R. Chen, T. M. Li, H. Merrick, R. F. Parrish, V. Bruno, A. Kwong, C. Stiso and D. J. Litman, *Clin. Chem.*, 1987, **33**, 1521–1525.
37 L. M. Vaughan, M. M. Weinberger, G. Milavetz, S. Tillson, E. Ellis, J. Jenne, S. J. Szefler, M. B. Wiener, K. Conboy and T. Shaughnessy, *et al.*, *Lancet*, 1986, **1**, 184–186.
38 V. Y. Liu, T. Y. Lin, W. Schrier, M. Allen and P. Singh, *Clin. Chem.*, 1993, **39**, 1948–1952.
39 M. P. Allen, A. DeLizza, U. Ramel, H. Jeong and P. Singh, *Clin. Chem.*, 1990, **36**, 1591–1597.
40 G. G. Lewis, M. J. DiTucci and S. T. Phillips, *Angew. Chem., Int. Ed.*, 2012, **51**, 12707–12710.
41 R. Hayes, *Cancer, Causes Control*, 1997, **8**, 371–385.
42 T. Menné and E. Nieboer, *Endeavour*, 1989, **13**, 117–122.
43 L. Järup, T. Bellander, C. Hogstedt and G. Spång, *Occup. Environ. Med.*, 1998, **55**, 755–759.
44 S.-C. Xu, M.-D. He, Y.-H. Lu, L. Li, M. Zhong, Y.-W. Zhang, Y. Wang, Z.-P. Yu and Z. Zhou, *J. Pineal Res.*, 2011, **51**, 426–433.
45 G. K. Balendiran, R. Dabur and D. Fraser, *Cell Biochem. Funct.*, 2004, **22**, 343–352.
46 I. Ceballos-Picot, V. Witko-Sarsat, M. Merad-Boudia, A. T. Nguyen, M. Thévenin, M. C. Jaudon, J. Zingraff, C. Verger, P. Jingers and B. Descamps-Latscha, *Free Radical Biol. Med.*, 1996, **21**, 845–853.
47 L. A. Herzenberg, S. C. De Rosa, J. G. Dubs, M. Roederer, M. T. Anderson, S. W. Ela, S. C. Deresinski and L. A. Herzenberg, *Proc. Natl. Acad. Sci. U. S. A.*, 1997, **94**, 1967–1972.
48 J. P. Richie Jr, *Exp. Gerontol.*, 1992, **27**, 615–626.
49 D. M. Townsend, K. D. Tew and H. Tapiero, *Biomed. Pharmacother.*, 2003, **57**, 145–155.
50 R. Ng, *Point Care*, 2008, **7**, 161 110.1097/1001.POC.0000335868.0000321077.c0000335860.
51 M. M. Mentele, J. Cunningham, K. Koehler, J. Volckens and C. S. Henry, *Anal. Chem.*, 2012, **84**, 4474–4480.
52 D. B. Gazda, J. S. Fritz and M. D. Porter, *Anal. Chim. Acta*, 2004, **508**, 53–59.
53 M. Stobiecka, K. Coopersmith and M. Hepel, *J. Colloid Interface Sci.*, 2010, **350**, 168–177.
54 A. Yu, J. Shang, F. Cheng, B. A. Paik, J. M. Kaplan, R. B. Andrade and D. M. Ratner, *Langmuir*, 2012, **28**, 11265–11273.
55 H. X. Li and L. J. Rothberg, *J. Am. Chem. Soc.*, 2004, **126**, 10958–10961.
56 H. Li and L. Rothberg, *Proc. Natl. Acad. Sci. U. S. A.*, 2004, **101**, 14036–14039.
57 J.-S. Lee, M. S. Han and C. A. Mirkin, *Angew. Chem.*, 2007, **119**, 4171–4174.
58 H. Wei, B. Li, J. Li, E. Wang and S. Dong, *Chem. Commun.*, 2007, 3735–3737.
59 Y. Zhou, Z. Yang and M. Xu, *Anal. Methods*, 2012, **4**, 2711–2714.

 